

ANALYSIS OF OFF-AXIS TENSION TEST OF WOOD SPECIMENS

Jen Y. Liu

Research General Engineer
U.S. Department of Agriculture
Forest Service
Forest Products Laboratory¹
One Gifford Pinchot Drive
Madison, WI 53705-2398

(Received March 2001)

ABSTRACT

This paper presents a stress analysis of the off-axis tension test of clear wood specimens based on orthotropic elasticity theory. The effects of Poisson's ratio and shear coupling coefficient on stress distribution are analyzed in detail. The analysis also provides a theoretical foundation for the selection of a 10° grain angle in wood specimens for the characterization of shear properties. The Tsai–Hill failure theory is then applied to derive a formula for predicting shear strength. Existing strength data for Sitka spruce (*Picea sitchensis* Carr.) were used in a numerical analysis. Because of the large discrepancies in published test data from different sources, the accuracy of the formula is limited to the data used to derive it. However, the procedures are believed to be accurate. The off-axis tension test is attractive mainly because of its economy and ease of application. This research promises to pave the way for the adoption of the off-axis tension test for characterizing the shear properties of clear wood by the practicing engineer once representative input data become available.

Keywords: Off-axis tension test, orthotropic elasticity, shear strength, tensile strength, Tsai–Hill failure theory.

INTRODUCTION

The off-axis tension test has become attractive for determining the shear properties of composite materials because of its relatively low cost and operational simplicity. Pagano and Halpin (1968) studied the problem of specimen end constraints and the effect of the length-to-width ratio. Wu and Thomas (1968) discussed a rotating clamp fixture design. The results of Pagano and Halpin (1968) were verified and extended by Richards et al. (1969) and Rizzo (1969). Chamis and Sinclair (1977) proposed a 10° off-axis tensile specimen for characterizing fiber–composite intralaminar shear.

More recently, Pindera and Herakovich (1986) studied the relation between end constraints and accurate determination of shear

modulus and the necessity of including shear coupling in stress analyses. Pierron and Vautrin (1996) discussed the use of oblique tabs proposed by Sun and Chung (1993). Pierron et al. (1998) then performed a whole-field assessment of the effects of end constraints on the strain field and reported that oblique tabbing can lead to a homogeneous strain field. Yoshihara and Ohta (2000) conducted an off-axis tension test for shear strength of Sitka spruce (*Picea sitchensis* Carr.) and other species. Their sample size was relatively small, nor did they apply any failure criteria to analyze their data. Consequently, their results seem to be somewhat inconclusive.

In the present study, we performed a detailed stress analysis for the off-axis tension test for clear Sitka spruce specimens to evaluate the effects of Poisson's ratio and shear coupling coefficient on stress distribution. We then applied the Tsai–Hill failure criterion using test data from Yoshihara and Ohta (2000), the Forest Products Laboratory (FPL 1999),

¹ The Forest Products Laboratory is maintained in cooperation with the University of Wisconsin. This article was written and prepared by U.S. Government employees on official time, and it is therefore in the public domain and not subject to copyright.

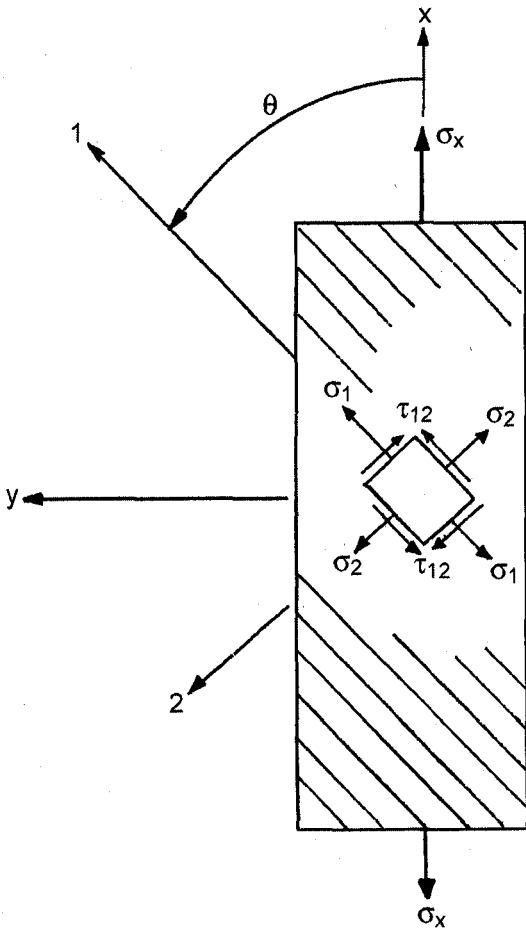


FIG. 1. Schematic of off-axis tension specimen. (x, y are geometrical axes; 1,2 are material axes.)

and Liu and Floeter (1984). A procedure to use the 10° off-axis tension test for the determination of clear wood shear strength is suggested.

STRESS-STRAIN RELATIONS

Let the 1-2 coordinate system represent the principal material axes and the x - y coordinate system the geometrical axes with angle q from the x axis to the 1 axis, as shown in Fig. 1. The normal stresses s_1 and s_2 in the 1 and 2 axes, respectively, and the shear stress t_6 or t_{12} in the 1-2 plane can be written as

$$\sigma_1 = \sigma_x m^2 \tag{1a}$$

$$\sigma_2 = \sigma_x n^2 \tag{1b}$$

$$\tau_6 = -\sigma_x mn \tag{1c}$$

where

$$m = \cos q \quad \text{and} \quad n = \sin q \tag{2}$$

The relations in Eq. (1) are independent of material properties; i.e., they are the same for isotropic or anisotropic materials.

For an anisotropic or orthotropic material such as wood, the applied stress s_x in Fig. 1 produces the following strains:

$$\epsilon_x = \frac{\sigma_x}{E_x} \quad \epsilon_y = -\frac{\nu_{xy}}{E_x} \sigma_x \quad \gamma_s = \frac{\eta_{xs}}{E_x} \sigma_x \tag{3}$$

In Eq. (3), the Poisson's ratio ν_{xy} , corresponding to stress in the x -direction and strain in the y -direction, is the negative ratio of the transverse strain e_y to the axial strain e_x . The shear coupling coefficient h_{xs} , corresponding to normal stress in the x -direction and shear strain in the x - y plane, is the ratio of the shear strain g_x or g_y to the axial strain e_x .

The strain components referred to the 1 and 2 axes can be expressed in terms of those referred to the x, y axes by the following transformation relations:

$$\begin{bmatrix} \epsilon_1 \\ \epsilon_2 \\ \frac{1}{2}\gamma_6 \end{bmatrix} = [T] \begin{bmatrix} \epsilon_x \\ \epsilon_y \\ \frac{1}{2}\gamma_s \end{bmatrix} \tag{4}$$

where the transformation matrix $[T]$ is given by

$$[T] = \begin{bmatrix} m^2 & n^2 & 2mn \\ n^2 & m^2 & -2mn \\ -mn & mn & m^2 - n^2 \end{bmatrix} \tag{5}$$

The stress-strain relations in the 1-2 coordinate system are

$$\begin{bmatrix} \sigma_1 \\ \sigma_2 \\ \tau_6 \end{bmatrix} = \begin{bmatrix} Q_{11} & Q_{12} & 0 \\ Q_{12} & Q_{22} & 0 \\ 0 & 0 & 2Q_{66} \end{bmatrix} \begin{bmatrix} \epsilon_1 \\ \epsilon_2 \\ \frac{1}{2}\gamma_6 \end{bmatrix} \tag{6}$$

The reduced stiffnesses Q_{11} , Q_{22} , Q_{12} , and Q_{66} can be related to the basic engineering constants E_1 , E_2 , G_{12} , and ν_{12} as follows:

$$\begin{aligned} Q_{11} &= \frac{E_1}{1 - \nu_{12}\nu_{21}} & Q_{22} &= \frac{E_2}{1 - \nu_{12}\nu_{21}} \\ Q_{12} &= \frac{\nu_{21}E_1}{1 - \nu_{12}\nu_{21}} = \frac{\nu_{12}E_2}{1 - \nu_{12}\nu_{21}} \\ Q_{66} &= G_{12} \end{aligned} \quad (7)$$

From Eqs. (3), (4), and (6) by means of Eqs. (5) and (7), we obtain expressions for \mathbf{s}_1 , \mathbf{s}_2 , and \mathbf{t}_6 in terms of the engineering constants, which should be equal to the corresponding expressions in Eq. (1). These expressions can be put in dimensionless form as follows:

$$\begin{aligned} \frac{\sigma_1}{\sigma_x} &= \frac{E_1}{E_x(1 - \nu_{12}\nu_{21})} \\ &\times [m^2 + \nu_{21}n^2 - \nu_{xy}(n^2 + \nu_{21}m^2) \\ &\quad + \eta_{xs}(1 - \nu_{21})mn] = m^2 \end{aligned} \quad (8a)$$

$$\begin{aligned} \frac{\sigma_2}{\sigma_x} &= \frac{E_2}{E_x(1 - \nu_{12}\nu_{21})} \\ &\times [\nu_{12}m^2 + n^2 - \nu_{xy}(\nu_{12}n^2 + m^2) \\ &\quad + \eta_{xs}(\nu_{12} - 1)mn] = n^2 \end{aligned} \quad (8b)$$

$$\begin{aligned} \frac{\tau_6}{\sigma_x} &= \frac{G_{12}}{E_x} [-2mn(1 + \nu_{xy}) + \eta_{xs}(m^2 - n^2)] \\ &= -mn \end{aligned} \quad (8c)$$

In Eq. (8), the transformed elasticity modulus E_x , the Poisson's ratio ν_{xy} , and the shear coupling coefficient \mathbf{h}_{xs} are as follows (Jones 1975):

$$\frac{1}{E_x} = \frac{1}{E_1}m^4 + \left(\frac{1}{G_{12}} - \frac{2\nu_{12}}{E_1}\right)m^2n^2 + \frac{1}{E_2}n^2 \quad (9)$$

$$\begin{aligned} \frac{\nu_{xy}}{E_x} &= \frac{\nu_{12}}{E_1}(m^4 + n^4) \\ &\quad - \left(\frac{1}{E_1} + \frac{1}{E_2} - \frac{1}{G_{12}}\right)m^2n^2 \end{aligned} \quad (10)$$

$$\begin{aligned} \frac{\eta_{xs}}{E_x} &= 2 \left[\left(\frac{1}{E_1} + \frac{\nu_{12}}{E_1} - \frac{1}{2G_{12}} \right) m^2 \right. \\ &\quad \left. - \left(\frac{1}{E_2} + \frac{\nu_{12}}{E_1} - \frac{1}{2G_{12}} \right) n^2 \right] mn \end{aligned} \quad (11)$$

TSAI-HILL FAILURE CRITERION

The Tsai-Hill criterion for orthotropic materials (Daniel and Ishai 1994) is

$$\frac{\sigma_1^2}{F_1^2} + \frac{\sigma_2^2}{F_2^2} + \frac{\tau_6^2}{F_6^2} - \frac{\sigma_1\sigma_2}{F_1^2} = 1 \quad (12)$$

in which F_1 , F_2 , and F_6 are the values of \mathbf{s}_1 , \mathbf{s}_2 , and \mathbf{t}_6 at failure, respectively, and the normal stress and strength in any one direction must be either tensile or compressive. Substituting Eq. (1) into Eq. (12) with the applied stress \mathbf{s}_x replaced by F_x , we obtain

$$\frac{1}{F_x^2} = \frac{m^4}{F_1^2} + \frac{n^4}{F_2^2} + \left(\frac{1}{F_6^2} - \frac{1}{F_1^2} \right) m^2n^2 \quad (13)$$

Note that F_x corresponding to any specified angle \mathbf{q} can be predicted once F_1 , F_2 , and F_6 are known. The Tsai-Hill theory allows for considerable interaction among the stress components \mathbf{s}_1 , \mathbf{s}_2 , and \mathbf{t}_6 . The requirement that each normal stress and the corresponding strength should be either tensile or compressive poses no problem because an off-axis tension test involves only tensile stresses and strengths.

RESULTS AND DISCUSSION

We obtained numerical results to demonstrate the effects of Poisson's ratio and shear coupling coefficient on stress distribution in defect-free Sitka spruce based on Eq. (8). Identifying the longitudinal axis with the 1 axis and the radial axis with the 2 axis, the basic engineering constants for Sitka spruce (Liu and Ross 1998) are $E_1 = 11,800$ MPa, $E_2 = 2,216$ MPa, $G_{12} = 910$ MPa, and $\nu_{12} = 0.37$. Using these values as input, E_x , ν_{xy} , and \mathbf{h}_{xs} , which are needed in Eq. (8), are first calculated.

Figure 2 presents the variation of the ratio

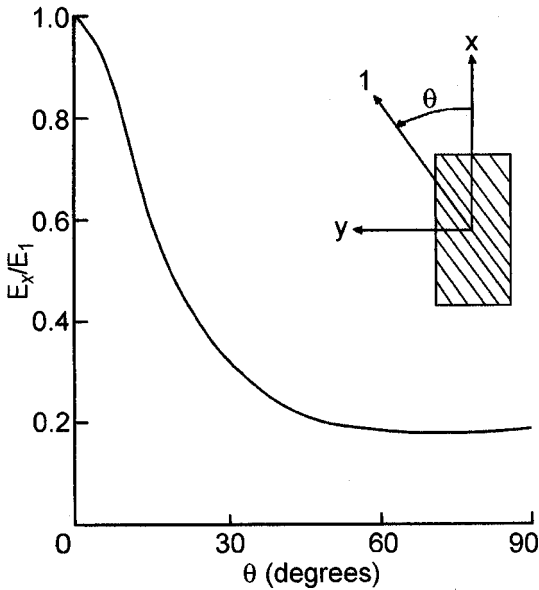


FIG. 2. Elasticity modulus of Sitka spruce as a function of grain angle. $E_1 = 11,800$ MPa, $E_2 = 2,216$ MPa, $G_{12} = 910$ MPa, and $\nu_{12} = 0.37$.

E_x/E_1 with \mathbf{q} . The maximum value occurs at $\mathbf{q} = 0^\circ$. It decreases drastically to $\mathbf{q} = 30^\circ$ and reaches a constant value of E_2/E_1 at about $\mathbf{q} = 55^\circ$. At $\mathbf{q} = 10^\circ$, the decrease in E_x is about 23% of E_1 .

Figure 3 shows that \mathbf{h}_{xs} is negative at $0^\circ \leq \mathbf{q} \leq 69^\circ$ with a minimum value of -1.42 at $\mathbf{q} = 15^\circ$. At $69^\circ < \mathbf{q} \leq 90^\circ$, \mathbf{h}_{xs} is positive with a maximum value of 0.04 at $\theta = 79^\circ$. The Poisson's ratio starts from 0.37 at $\mathbf{q} = 0^\circ$, reaches a maximum value of 0.47 at $\mathbf{q} = 25^\circ$, and drops to 0.07 at $\mathbf{q} = 90^\circ$.

Using these data, we found that all of equations (8) are satisfied for any value of \mathbf{q} . We then plotted from Eq. (8a) the sum of terms containing \mathbf{h}_{xs} , the sum of terms containing ν_{xy} , and the total of all terms, i.e., m^2 , versus \mathbf{q} (Fig. 4). As Fig. 4 shows, \mathbf{h}_{xs} has a stronger effect than ν_{xy} on $\mathbf{s}_1/\mathbf{s}_x$ at $3^\circ \leq \mathbf{q} \leq 45^\circ$. Beyond that range, the reverse is true.

Figure 5 shows the results from Eq. (8b). Here the sum of terms containing \mathbf{h}_{xs} has the same sign as the total, n^2 , while that of ν_{xy} has the opposite sign in the range of $\mathbf{q} < 67^\circ$. Be-

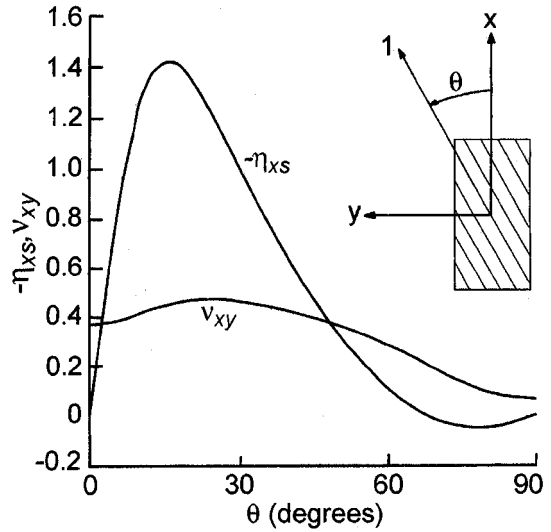


FIG. 3. Shear coupling coefficient and Poisson's ratio of Sitka spruce as a function of grain angle.

yond that range, both have insignificant effects on the total.

The ratio of $\mathbf{t}_\theta/\mathbf{s}_x$ in Eq. (8c) plotted in Fig. 6 reveals that up to $\mathbf{q} \gg 10^\circ$, the total mn is only slightly above the sum of terms containing \mathbf{h}_{xs} and the two vary linearly with \mathbf{q} , indicating that \mathbf{h}_{xs} has a predominant effect on \mathbf{t}_θ when $\mathbf{q} = 10^\circ$. Assuming that when \mathbf{s}_x increases to cause material to fail and the same

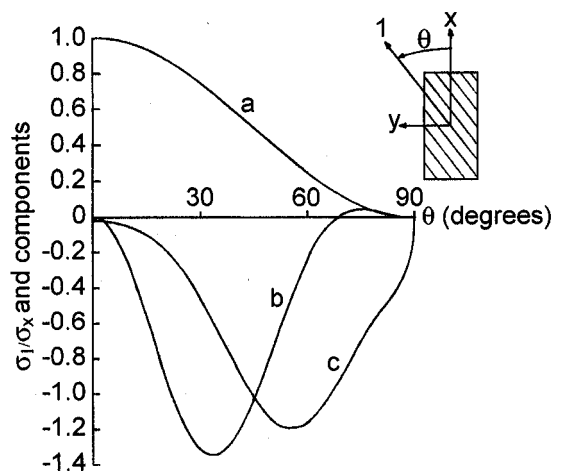


FIG. 4. Variations of $\mathbf{s}_1/\mathbf{s}_x$ with \mathbf{q} showing effects of \mathbf{h}_{xs} and ν_{xy} (Eq. 8a). a = m^2 , b = terms containing \mathbf{h}_{xs} , c = terms containing ν_{xy} .

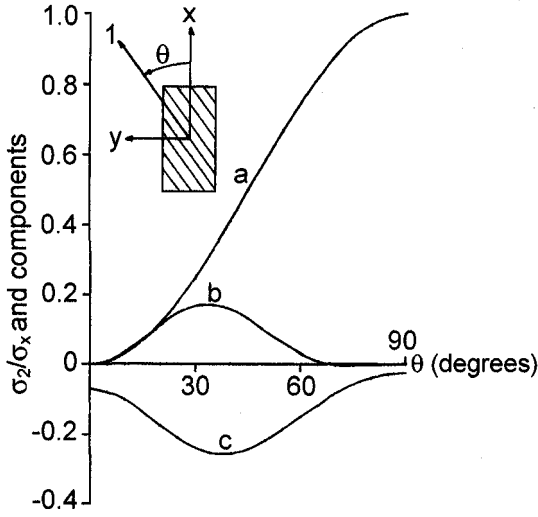


FIG. 5. Variations of (s_2/s_x) with q showing effects of h_{xy} and v_{xy} (Eq. 8b). a = n^2 , b = terms containing h_{xy} , c = terms containing v_{xy}

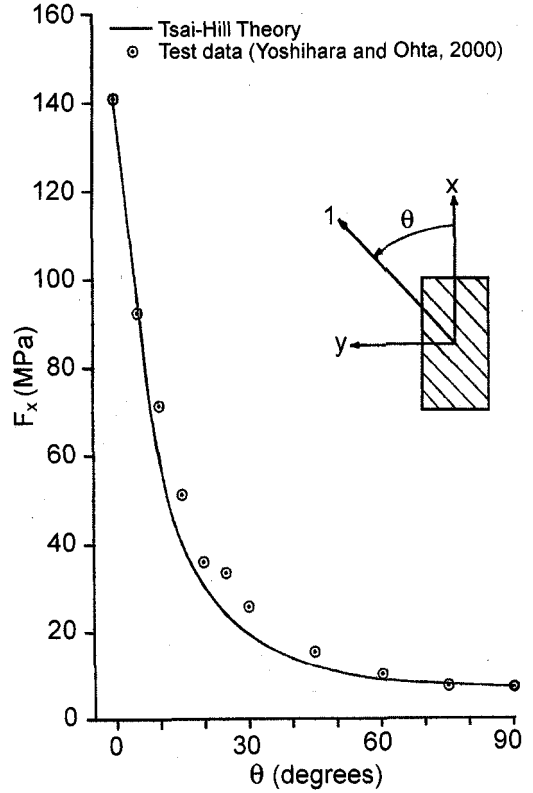


FIG. 7. Failure curve based on Tsai-Hill theory for $F_1 = 141$ MPa, $F_2 = 7.4$ MPa, and $F_6 = 11.3$ MPa and test data for Yoshihara and Ohta (2000).

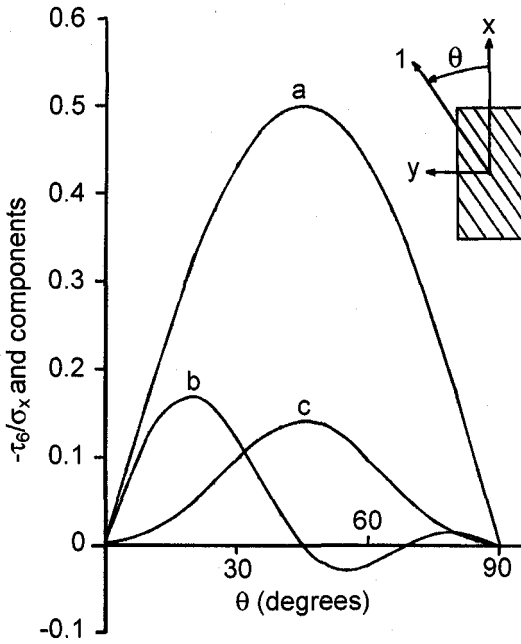


FIG. 6. Variations of $-t_6/s_x$ with q showing effects of h_{xy} and v_{xy} (Eq. 8c). a = m , b = terms containing h_{xy} , c = terms containing v_{xy} .

relation between s_x and t_6 still holds, the value of t_6 at that instant must have a definite relation with its value at the yield limit.

The Tsai-Hill failure criterion in Eq. (13) is based on assumptions of homogeneity (Perkins, Jr. 1972) and linear stress-strain behavior to failure as are almost all other macromechanical failure theories. It shows that for the prediction of failure load F_x corresponding to any specified value of q , only the values of F_1 , F_2 , and F_6 are needed. Yoshihara and Ohta (2000) recently published these values for Sitka spruce as $F_1 = 141$ MPa, $F_2 = 7.4$ MPa, and $F_6 = 11.3$ MPa. Using these values in Eq. (13), the failure curve obtained is shown in Fig. 7 together with the test data of F_x at several q values. Within the range $110^\circ < q < 75^\circ$, the test data are significantly above the predicted values. With the F_x values from the

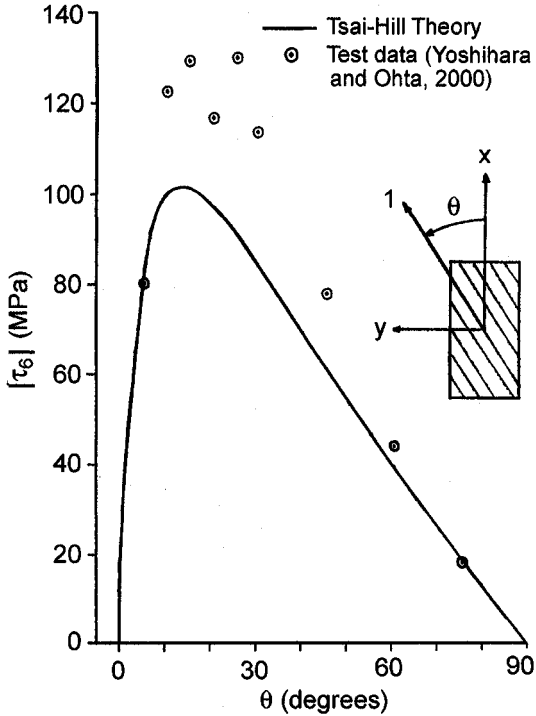


FIG. 8. Variation of $|\tau_6|$ with q at occurrence of F_x .

Tsai-Hill theory and the test data in Fig. 7 representing the corresponding value of s_x in Eq. (1c), the shear stresses $|\tau_6|$ at failure are plotted in Fig. 8. (Note: In the Tsai-Hill theory, the sign for τ_6 makes no difference. We therefore use its absolute value.) At $q = 10^\circ$, $|\tau_6|$ is only about 1.2% less than its maximum value, which occurs at $q \gg 13^\circ$, based on the Tsai-Hill theory. However, the test data are more prominently above the theoretical predictions at $10^\circ < q < 45^\circ$. It is against any theory for $|\tau_6|$ to be larger than F_6 in an off-axis tension test. When that happens, the test facilities, specimen conditions, sample size, and other variables may all need to be reexamined. However, if we use the predicted value of $F_x = 58.57$ MPa at $q = 10^\circ$ and substitute it into Eq. (1c) for s_x , we obtain $|\tau_6| = 10$ MPa, which is about 13% less than $F_6 = 11.3$ MPa, and seems to be reasonable. So, the important question is how reliable are the F_1 , F_2 , and F_6 values that were used in Eq. (13).

In the *Wood Handbook* (FPL 1999), F_1 , F_2 ,

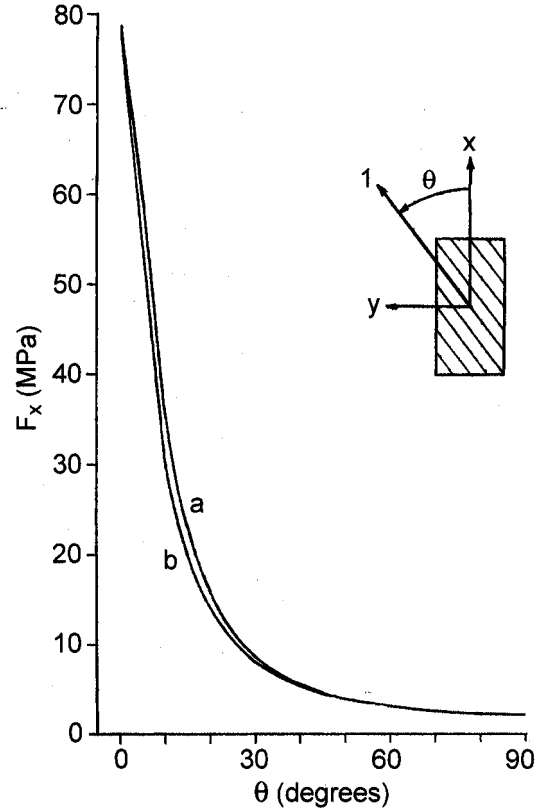


FIG. 9. Failure curve based on Tsai-Hill theory for two sets of F_x values: (a) $F_1 = 78.3$ MPa, $F_2 = 2.55$ MPa, and $F_6 = 7.93$ MPa (FPL 1999). (b) $F_1 = 78.3$ MPa, $F_2 = 2.55$ MPa, and $F_6 = 6.25$ MPa (Liu and Floeter 1984).

and F_6 values for Sitka spruce are 78.3, 2.55, and 7.93 MPa, respectively, which are considerably lower than the values found by Yoshihara and Ohta (2000).² Using these values in Eq. (13), we obtain $F_x = 36.43$ MPa at $q = 10^\circ$ (Fig. 9). The corresponding value of $|\tau_6|$ from Eq. (1c) is 6.23 MPa, which is about 27% less than $F_6 = 7.93$ MPa.

Liu and Floeter (1984) reported that $F_6 = 6.25$ MPa for Sitka spruce. Using $F_1 = 78.3$ MPa, $F_2 = 2.55$ MPa, and $F_6 = 6.25$ MPa, and following the same steps as described in the preceding text, we obtain $F_x = 31.05$ MPa at $q = 10^\circ$ and $|\tau_6| = 5.31$ MPa, which is about

²The *Wood Handbook* F_1 value is adjusted based on data from dry specimens.

18% less than $F_6 = 6.25$ MPa. Note the close proximity of the two failure curves in Fig. 9.

We are now ready to discuss the procedures to determine F_6 from the 10° off-axis tension test. Assuming the set of data $F_1 = 141$ MPa, $F_2 = 7.4$ MPa, and $F_6 = 11.3$ MPa is valid, we have found that $F_x(\mathbf{q} = 10^\circ) = 31.05$ MPa and $|t_6| = 5.31$ MPa, which is about 18% less than $F_6 = 6.25$ MPa. Since 13% and 18% are close to one another, we select their mean, which is about 15%. We therefore obtain

$$F_6 \approx F_x(\theta = 10^\circ) \times \sin 10^\circ \cos 10^\circ \times 1.15 \\ = F_x(\theta = 10^\circ) \times 0.2 \quad (14)$$

Also, from these two sets of data, we find $F_x(\mathbf{q} = 10^\circ) \gg 0.4 \times F_1$. We can replace Eq. (14) by

$$F_6 = 0.08 \times F_1 \quad (15)$$

Our discussion is based on the Tsai–Hill theory and limited test data for Sitka spruce from different sources. Although there are considerable discrepancies between the two sets of test data, the formulas seem to be valid for both. The discrepancies may need to be reconciled, but the procedures presented are believed to be useful in applying the off-axis tension test for the characterization of wood shear properties.

CONCLUSIONS

1. In an off-axis tension test of clear wood specimens, at a 10° grain angle, the shear stress in the principal material plane is due mainly to the shear coupling coefficient.
2. In applying the Tsai–Hill theory for tensile strength prediction of wood at any grain angle, the strength data in the principal material axes and plane must be reliable to produce accurate results.
3. The 10° off-axis tension test can be used to predict clear wood shear strength in a principal material plane of wood.
4. A formula has been derived for shear

strength prediction of Sitka spruce based on input data in the literature.

REFERENCES

- CHAMIS, C. C., AND J. H. SINCLAIR. 1997. Ten degree off-axis test for shear properties in fiber composites. *Exp. Mech.* 17(9):339–346.
- DANIEL, I. M., AND O. ISHAI. 1994. *Engineering mechanics of composite materials*. Oxford Univ. Press, Oxford, UK. 395 pp.
- FOREST PRODUCTS LABORATORY (FPL). 1999. *Wood handbook. Wood as an engineering material*. Gen Tech Rep. FPL-GRT-113. USDA, Forest Serv., Forest Products Lab., Madison, WI. 463 pp.
- JONES, R. M. 1975. *Mechanics of composite materials*. Scripta Book Co., Washington, DC. 344 pp.
- LIU, J. Y., AND L. H. FLOETER. 1984. Shear strength in principal plane of wood. *J. Eng. Mech.* 110(6):930–936.
- , AND R. J. ROSS. 1998. Wood property variation with grain slope. Pages 1351–1354 in *Proc. 12th Engineering Mechanics Conf.*, American Society of Civil Engineers, La Jolla, CA.
- PAGANO, N. J., AND J. C. HALPIN. 1968. Influence of end constraint in the testing of anisotropic bodies. *J. Comp. Mat.* 2(1):18–31.
- PERKINS, JR., R. W. 1972. On the mechanical response of materials with cellular and finely layered internal structures. In B. A. Jayne, ed. *Theory and design of wood and fiber composite materials*. Syracuse University Press, Syracuse, NY.
- PIERON, F., AND A. VAUTRIN. 1996. The 10° off-axis tensile test: A critical approach. *Comp. Sci. Technol.* 56(4): 483–488.
- , E. ALLOBA, Y. SURREL, AND A. VAUTRIN. 1998. Whole-field assessment of the effects of boundary conditions on the strain field in off-axis tensile testing of unidirectional composites. *Comp. Sci. Technol.* 58(12): 1939–1947.
- PINDERA, M.-J., AND C. T. HERAKOVICH. 1986. Shear characterization of unidirectional composites with the off-axis tension test. *Exp. Mech.* 26(1):103–112.
- RICHARDS, G. L., T. P. AIRHART, AND J. E. ASHTON. 1969. Off-axis tensile testing. *J. Comp. Mat.* 3:586–589.
- RIZZO, R. R. 1969. More on the influence of end constraints on oo-axis tensile tests. *J. Comp. Mat.* 3:202–219.
- SUN, C. T., AND I. CHUNG. 1993. An oblique end-tab design for testing off-axis composite specimens. *Composites* 24(8):619–623.
- WU, E. M., AND R. L. THOMAS. 1968. Off-axis test of a composite. *J. Comp. Mat.* 2(4): 523–526.
- YOSHIHARA, H. AND M. OHTA. 2000. Estimation of the shear strength of wood by uniaxial-tension tests of off-axis specimens. *J. Wood Sci.* 46(2):159–163.